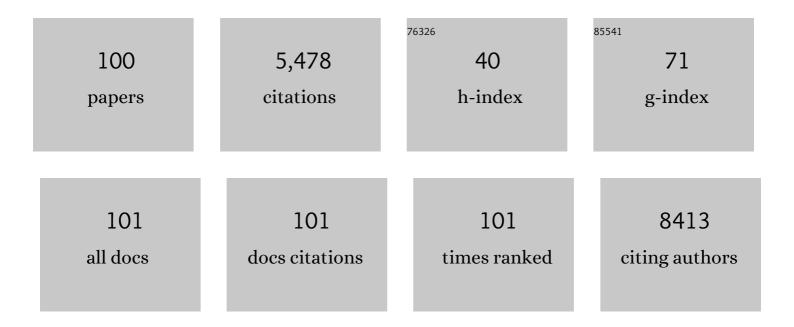
Baoyou Geng

List of Publications by Year in descending order

Source: https://exaly.com/author-pdf/4146814/publications.pdf Version: 2024-02-01



RAOVOU GENC

#	Article	IF	CITATIONS
1	Non-enzymatic electrochemical sensing of glucose. Mikrochimica Acta, 2013, 180, 161-186.	5.0	427
2	High supercapacitor and adsorption behaviors of flower-like MoS ₂ nanostructures. Journal of Materials Chemistry A, 2014, 2, 15958-15963.	10.3	283
3	Facile Subsequently Light-Induced Route to Highly Efficient and Stable Sunlight-Driven Agâ^'AgBr Plasmonic Photocatalyst. Langmuir, 2010, 26, 18723-18727.	3.5	257
4	A Reliable Aerosolâ€6prayâ€Assisted Approach to Produce and Optimize Amorphous Metal Oxide Catalysts for Electrochemical Water Splitting. Angewandte Chemie - International Edition, 2014, 53, 7547-7551.	13.8	234
5	Titania supported synergistic palladium single atoms and nanoparticles for room temperature ketone and aldehydes hydrogenation. Nature Communications, 2020, 11, 48.	12.8	223
6	Massâ€Production of Mesoporous MnCo ₂ O ₄ Spinels with Manganese(IV)―and Cobalt(II)â€Rich Surfaces for Superior Bifunctional Oxygen Electrocatalysis. Angewandte Chemie - International Edition, 2017, 56, 14977-14981.	13.8	184
7	Facile one-pot synthesis of novel hierarchical Bi2O3/Bi2S3 nanoflower photocatalyst with intrinsic p-n junction for efficient photocatalytic removals of RhB and Cr(VI). Journal of Hazardous Materials, 2020, 381, 120942.	12.4	180
8	Superior performance asymmetric supercapacitors based on ZnCo ₂ O ₄ @MnO ₂ core–shell electrode. Journal of Materials Chemistry A, 2015, 3, 5442-5448.	10.3	158
9	A facile solution chemical route to self-assembly of CuS ball-flowers and their application as an efficient photocatalyst. CrystEngComm, 2010, 12, 144-149.	2.6	157
10	Scalable Dry Production Process of a Superior 3D Netâ€Like Carbonâ€Based Iron Oxide Anode Material for Lithiumâ€Ion Batteries. Angewandte Chemie - International Edition, 2017, 56, 12649-12653.	13.8	126
11	A facile coordination compound precursor route to controlled synthesis of Co3O4 nanostructures and their room-temperature gas sensing properties. Journal of Materials Chemistry, 2008, 18, 4977.	6.7	122
12	A template-free route to a Fe3O4–Co3O4 yolk–shell nanostructure as a noble-metal free electrocatalyst for ORR in alkaline media. Journal of Materials Chemistry, 2012, 22, 19132.	6.7	116
13	Fabrication of FeNi hydroxides double-shell nanotube arrays with enhanced performance for oxygen evolution reaction. Applied Catalysis B: Environmental, 2020, 261, 118193.	20.2	99
14	Facile synthesis of Fe/Ni bimetallic oxide solid-solution nanoparticles with superior electrocatalytic activity for oxygen evolution reaction. Nano Research, 2015, 8, 3815-3822.	10.4	94
15	Hierarchical structures composed of MnCo ₂ O ₄ @MnO ₂ core–shell nanowire arrays with enhanced supercapacitor properties. Dalton Transactions, 2016, 45, 572-578.	3.3	88
16	Construction of unique Co ₃ O ₄ @CoMoO ₄ core/shell nanowire arrays on Ni foam by the action exchange method for high-performance supercapacitors. Journal of Materials Chemistry A, 2015, 3, 14578-14584.	10.3	84
17	A novel gelatin-guided mesoporous bowknot-like Co ₃ O ₄ anode material for high-performance lithium-ion batteries. Journal of Materials Chemistry A, 2017, 5, 5342-5350.	10.3	84
18	Heterostructural NiFe-LDH@Ni3S2 nanosheet arrays as an efficient electrocatalyst for overall water splitting. Electrochimica Acta, 2019, 318, 42-50.	5.2	84

#	Article	IF	CITATIONS
19	Well-Constructed Single-Layer Molybdenum Disulfide Nanorose Cross-Linked by Three Dimensional-Reduced Graphene Oxide Network for Superior Water Splitting and Lithium Storage Property. Scientific Reports, 2015, 5, 8722.	3.3	79
20	Ag–Au bimetallic nanostructures: co-reduction synthesis and their component-dependent performance for enzyme-free H2O2 sensing. Journal of Materials Chemistry A, 2013, 1, 7111.	10.3	73
21	Hierarchical NiMn ₂ O ₄ @CNT nanocomposites for high-performance asymmetric supercapacitors. RSC Advances, 2015, 5, 24607-24614.	3.6	73
22	Versatile Electronic and Magnetic Properties of SnSe ₂ Nanostructures Induced by the Strain. Journal of Physical Chemistry C, 2014, 118, 9251-9260.	3.1	68
23	3D porous gear-like copper oxide and their high electrochemical performance as supercapacitors. CrystEngComm, 2013, 15, 7657.	2.6	63
24	Ultrathin porous nickel–cobalt hydroxide nanosheets for high-performance supercapacitor electrodes. RSC Advances, 2015, 5, 17007-17013.	3.6	62
25	Massâ€Production of Mesoporous MnCo ₂ O ₄ Spinels with Manganese(IV)―and Cobalt(II)â€Rich Surfaces for Superior Bifunctional Oxygen Electrocatalysis. Angewandte Chemie, 2017, 129, 15173-15177.	2.0	61
26	Self-assembly fabrication of 3D porous quasi-flower-like ZnO nanostrip clusters for photodegradation of an organic dye with high performance. CrystEngComm, 2011, 13, 2137.	2.6	57
27	Oxygen Vacancy–Enhanced Electrocatalytic Performances of TiO ₂ Nanosheets toward N ₂ Reduction Reaction. Advanced Materials Interfaces, 2019, 6, 1901034.	3.7	54
28	Three-dimensional NiCo ₂ O ₄ @NiMoO ₄ core/shell nanowires for electrochemical energy storage. Journal of Materials Chemistry A, 2015, 3, 12069-12075.	10.3	51
29	Porous Mn ₂ O ₃ : A Lowâ€Cost Electrocatalyst for Oxygen Reduction Reaction in Alkaline Media with Comparable Activity to Pt/C. Chemistry - A European Journal, 2016, 22, 9909-9913.	3.3	49
30	Fe–Ni Layered Double Hydroxide Arrays with Homogeneous Heterostructure as Efficient Electrocatalysts for Overall Water Splitting. ACS Sustainable Chemistry and Engineering, 2019, 7, 15073-15079.	6.7	49
31	Ultrastable and efficient H ₂ production <i>via</i> membrane-free hybrid water electrolysis over a bifunctional catalyst of hierarchical Mo–Ni alloy nanoparticles. Journal of Materials Chemistry A, 2019, 7, 16501-16507.	10.3	49
32	A facile and efficient strategy to gram-scale preparation of composition-controllable Ni-Fe LDHs nanosheets for superior OER catalysis. Electrochimica Acta, 2017, 225, 303-309.	5.2	46
33	Egg albumin as a nanoreactor for growing single-crystalline Fe3O4 nanotubes with high yields. Chemical Communications, 2008, , 5773.	4.1	45
34	Gas template-assisted spray pyrolysis: A facile strategy to produce porous hollow Co3O4 with tunable porosity for high-performance lithium-ion battery anode materials. Nano Research, 2018, 11, 1490-1499.	10.4	45
35	Atomically Dispersed Pt/Metal Oxide Mesoporous Catalysts from Synchronous Pyrolysis–Deposition Route for Water–Gas Shift Reaction. Chemistry of Materials, 2018, 30, 5534-5538.	6.7	44
36	ZnO nanorods/ZnSe heteronanostructure arrays with a tunable microstructure of ZnSe shell for visible light photocatalysis. Journal of Materials Chemistry A, 2014, 2, 17502-17510.	10.3	43

#	Article	IF	CITATIONS
37	Magnetic Nanotubes: Synthesis, Properties, and Applications. Critical Reviews in Solid State and Materials Sciences, 2012, 37, 75-93.	12.3	42
38	Aerosol-spray diverse mesoporous metal oxides from metal nitrates. Scientific Reports, 2015, 5, 9923.	3.3	42
39	Colloidal Synthesis of Mo–Ni Alloy Nanoparticles as Bifunctional Electrocatalysts for Efficient Overall Water Splitting. Advanced Materials Interfaces, 2018, 5, 1800359.	3.7	42
40	Dual-Mode Long-Lived Luminescence of Mn ²⁺ -Doped Nanoparticles for Multilevel Anticounterfeiting. ACS Applied Materials & Interfaces, 2019, 11, 30146-30153.	8.0	42
41	Simultaneous tunable structure and composition of PtAg alloyed nanocrystals as superior catalysts. Nanoscale, 2016, 8, 14971-14978.	5.6	40
42	Modified Kirkendall effect for fabrication of magnetic nanotubes. Chemical Communications, 2010, 46, 1899-1901.	4.1	38
43	Facile Growth of High-Yield Gold Nanobipyramids Induced by Chloroplatinic Acid for High Refractive Index Sensing Properties. Scientific Reports, 2016, 6, 36706.	3.3	38
44	Excellent lithium ion storage property of porous MnCo ₂ O ₄ nanorods. RSC Advances, 2016, 6, 23074-23084.	3.6	38
45	A multi-interfacial FeOOH@NiCo ₂ O ₄ heterojunction as a highly efficient bifunctional electrocatalyst for overall water splitting. Nanoscale, 2020, 12, 19404-19412.	5.6	38
46	Low-cost and highly efficient composite visible light-driven Ag–AgBr/γ-Al2O3 plasmonic photocatalyst for degrading organic pollutants. Catalysis Science and Technology, 2012, 2, 1269.	4.1	36
47	Mesoporous spherical Li4Ti5O12/TiO2 composites as an excellent anode material for lithium-ion batteries. Electrochimica Acta, 2016, 212, 41-46.	5.2	36
48	Hollow porous carbon spheres doped with a low content of Co3O4 as anode materials for high performance lithium-ion batteries. Electrochimica Acta, 2019, 317, 562-569.	5.2	35
49	Open N-doped carbon coated porous molybdenum phosphide nanorods for synergistic catalytic hydrogen evolution reaction. Nano Research, 2022, 15, 1824-1830.	10.4	35
50	Controllable synthesis of silver nanodendrites on copper rod and its application to hydrogen peroxide and glucose detection. CrystEngComm, 2013, 15, 1173-1178.	2.6	34
51	Engineering of Hollow PdPt Nanocrystals via Reduction Kinetic Control for Their Superior Electrocatalytic Performances. ACS Applied Materials & Interfaces, 2018, 10, 29543-29551.	8.0	31
52	Hydrothermal Synthesis of a rGO Nanosheet Enwrapped NiFe Nanoalloy for Superior Electrocatalytic Oxygen Evolution Reactions. Chemistry - A European Journal, 2016, 22, 14480-14483.	3.3	29
53	Synchronous constructing ion channels and confined space of Co3O4 anode for high-performance lithium-ion batteries. Nano Research, 2022, 15, 6192-6199.	10.4	29
54	Defectâ€Driven Enhancement of Electrochemical Oxygen Evolution on Fe–Co–Al Ternary Hydroxides. ChemSusChem, 2019, 12, 2564-2569.	6.8	28

#	Article	IF	CITATIONS
55	Highly dispersed Cu atoms in MOF-derived N-doped porous carbon inducing Pt loads for superior oxygen reduction and hydrogen evolution. Chemical Engineering Journal, 2021, 426, 130749.	12.7	28
56	Selective Reduction–Oxidation Strategy to the Conductivity-Enhancing Ag-Decorated Co-Based 2D Hydroxides as Efficient Electrocatalyst in Oxygen Evolution Reaction. ACS Sustainable Chemistry and Engineering, 2018, 6, 13420-13426.	6.7	27
57	Pt Nanoparticles Supported on N-Doped Porous Carbon Derived from Metal–Organic Frameworks for Oxygen Reduction. ACS Applied Nano Materials, 2020, 3, 5698-5705.	5.0	27
58	Sandwich shelled TiO ₂ @Co ₃ O ₄ @Co ₃ O ₄ /C hollow spheres as anode materials for lithium ion batteries. Chemical Communications, 2021, 57, 1786-1789.	4.1	27
59	Self-Supported CoFe-P Nanosheets as a Bifunctional Catalyst for Overall Water Splitting. ACS Applied Nano Materials, 2021, 4, 12083-12090.	5.0	27
60	Vesicular Li3V2(PO4)3/C hollow mesoporous microspheres as an efficient cathode material for lithium-ion batteries. Nano Research, 2019, 12, 1937-1942.	10.4	26
61	High-Density Pd Nanorod Arrays on Au Nanocrystals for High-Performance Ethanol Electrooxidation. ACS Applied Materials & Interfaces, 2019, 11, 20117-20124.	8.0	26
62	Dispersion and support dictated properties and activities of Pt/metal oxide catalysts in heterogeneous CO oxidation. Nano Research, 2021, 14, 4841-4847.	10.4	26
63	Ni2+/surfactant-assisted route to porous α-Fe2O3 nanoarchitectures. Nanoscale, 2012, 4, 1671.	5.6	25
64	Hydrothermal route to twinned-hemisphere-like CuO architectures with selective adsorption performance. CrystEngComm, 2012, 14, 3677.	2.6	24
65	Mesocrystal precursor transformation strategy for synthesizing ordered hierarchical hollow TiO2 nanobricks with enhanced photocatalytic property. CrystEngComm, 2014, 16, 2061.	2.6	24
66	Coralloid SnO2 with hierarchical structure and their application as recoverable gas sensors for the detection of benzaldehyde/acetone. Materials Chemistry and Physics, 2010, 122, 30-34.	4.0	23
67	Ge@C core–shell nanostructures for improved anode rate performance in lithium-ion batteries. RSC Advances, 2015, 5, 17070-17075.	3.6	23
68	Stick-like titania precursor route to MTiO3 (M = Sr, Ba, and Ca) polyhedra. CrystEngComm, 2012, 14, 2959.	2.6	22
69	Scalable Dry Production Process of a Superior 3D Netâ€Like Carbonâ€Based Iron Oxide Anode Material for Lithiumâ€Ion Batteries. Angewandte Chemie, 2017, 129, 12823-12827.	2.0	21
70	One-step synthesis and morphology evolution of luminescent Eu2+ doped strontium aluminate nanostructures. CrystEngComm, 2010, 12, 2722.	2.6	20
71	A room-temperature chemical route to homogeneous core–shell Cu2O structures and their application in biosensors. CrystEngComm, 2011, 13, 697-701.	2.6	20
72	CdS urchin-like microspheres/α-Fe2O3 and CdS/Fe3O4 nanoparticles heterostructures with improved photocatalytic recycled activities. Journal of Colloid and Interface Science, 2014, 426, 83-89.	9.4	20

#	Article	IF	CITATIONS
73	Constructing an interspace in MnO@NC microspheres for superior lithium ion battery anodes. Chemical Communications, 2021, 57, 10951-10954.	4.1	20
74	"Re-growth Etching―to Large-sized Porous Gold Nanostructures. Scientific Reports, 2013, 3, 2377.	3.3	19
75	Freeze-drying assisted biotemplated route to 3D mesoporous Na ₃ V ₂ (PO ₄) ₃ @NC composites as cathodes with high performance for sodium-ion batteries. Chemical Communications, 2020, 56, 11961-11964.	4.1	19
76	Shell structure-enhanced electrocatalytic performance of Au–Pt core–shell catalyst. CrystEngComm, 2013, 15, 2133.	2.6	17
77	Size-controllable synthesis of amorphous GeO _x hollow spheres and their lithium-storage electrochemical properties. RSC Advances, 2016, 6, 15952-15959.	3.6	17
78	A general gelatin-assisted strategy to hierarchical porous transition metal oxides with excellent lithium-ion storage. Electrochimica Acta, 2018, 279, 66-73.	5.2	17
79	Metal–Organic Framework-Derived Biln Bimetallic Oxide Nanoparticles Embedded in Carbon Networks for Efficient Electrochemical Reduction of CO ₂ to Formate. Inorganic Chemistry, 2022, 61, 12003-12011.	4.0	17
80	Delivery of Highly Active Nobleâ€Metal Nanoparticles into Microspherical Supports by an Aerosolâ€ S pray Method. Chemistry - A European Journal, 2015, 21, 13291-13296.	3.3	15
81	Au/Pt co-loaded ultrathin TiO ₂ nanosheets for photocatalyzed H ₂ evolution by the synergistic effect of plasmonic enhancement and co-catalysis. RSC Advances, 2015, 5, 98254-98259.	3.6	15
82	Hierarchical ZnO@MnO2@PPy ternary core–shell nanorod arrays: an efficient integration of active materials for energy storage. RSC Advances, 2015, 5, 39864-39869.	3.6	15
83	Low cost visible light driven plasmonic Ag–AgBr/BiVO ₄ system: fabrication and application as an efficient photocatalyst. RSC Advances, 2015, 5, 39651-39656.	3.6	15
84	Morphology-controllable synthesis of 3D firecracker-like ZnO nanoarchitectures for high catalytic performance. CrystEngComm, 2015, 17, 1121-1128.	2.6	13
85	Morphology Engineering of Au/(PdAg alloy) Nanostructures for Enhanced Electrocatalytic Ethanol Oxidation. Particle and Particle Systems Characterization, 2018, 35, 1800258.	2.3	13
86	Solubility-dependent gelatination toward N-doped SnOx/C deriving from commercial SnO2 for the ultrastable lithium storage. Journal of Power Sources, 2019, 441, 227172.	7.8	13
87	Hexamethylenetetramine induced multidimensional defects in Co ₂ P nanosheets for efficient alkaline hydrogen evolution. Chemical Communications, 2022, 58, 6352-6355.	4.1	13
88	Kinetic manipulation of the morphology evolution of FePO4 microcrystals: from rugbies to porous microspheres. CrystEngComm, 2009, 11, 2510.	2.6	12
89	A facile sonochemical route to morphology controlled nickel complex mesostructures. CrystEngComm, 2009, 11, 1317.	2.6	10
90	Synthesis of Ag/Ag ₂ CO ₃ heterostructures with high length–diameter ratios for excellent photoactivity and anti-photocorrosion. RSC Advances, 2016, 6, 103938-103943.	3.6	9

#	Article	IF	CITATIONS
91	Branched twinned Au nanostructures: facile hydrothermal reduction fabrication, growth mechanism and electrochemical properties. CrystEngComm, 2012, 14, 6581.	2.6	8
92	Simultaneous and Reversible Triggering of the Phase Transfer and Luminescence Change of Amidine-Modified Carbon Dots by CO ₂ . ACS Applied Materials & Interfaces, 2019, 11, 22851-22857.	8.0	7
93	Self-assembled porous ceria nanostructures with excellent water solubility and antioxidant properties. RSC Advances, 2016, 6, 45957-45962.	3.6	5
94	Plasmonic Band Tunable (Au Nanocrystal)/SnO ₂ Core/Shell Hybrids for Photothermal Therapy. Particle and Particle Systems Characterization, 2018, 35, 1800238.	2.3	5
95	Perovskite phase formation, microstructure and improvement of dielectric properties in iron-containing ferroelectrics. Physica Status Solidi (A) Applications and Materials Science, 2006, 203, 2538-2545.	1.8	4
96	Water Splitting Catalysts: Colloidal Synthesis of Mo-Ni Alloy Nanoparticles as Bifunctional Electrocatalysts for Efficient Overall Water Splitting (Adv. Mater. Interfaces 13/2018). Advanced Materials Interfaces, 2018, 5, 1870063.	3.7	4
97	In Situ Electrochemical Route to Bromide Anion-Adsorbed Coral-like Porous Silver Microspheres Achieving Highly Selective Electroreduction of CO ₂ to CO over a Wide Potential Range. ACS Sustainable Chemistry and Engineering, 2021, 9, 6756-6763.	6.7	4
98	Synergistic melamine intercalation and Zn(NO ₃) ₂ activation of N-doped porous carbon supported Fe/Fe ₃ O ₄ for efficient electrocatalytic oxygen reduction. RSC Advances, 2022, 12, 15705-15712.	3.6	4
99	Fabrication of ZnSe hexagonal prism with pyramid end through the chemical vapour deposition route. CrystEngComm, 2011, 13, 668-673.	2.6	3
100	Ultrathinâ€Branched Pt Grown on Quasiâ€Sphere Pd with Enhanced Electrocatalytic Performances. ChemistrySelect, 2018, 3, 1531-1536.	1.5	0